SLAMMING PRESSURES ON A MEGA YACHT

BY MEANS OF RANSE SIMULATIONS

Order:	MTG 367-636
Project title:	Berechnung der Extremlasten an einer 70 m Megajacht
Client:	Germanischer Lloyd
Contractor:	MTG Marinetechnik GmbH, Hamburg
Author:	Dr.-Ing. Rodrigo Azcueta
Date:	27th June 2003

1. INTRODUCTION

The motivation of the present work was twofold:

1- to determine the slamming pressures on a mega yacht built in Germany and currently sailing in mediterranean waters. This is required to dimension some of the panels at the flared bow which had suffered damage in the early voyages.

2- to compare the slamming pressures computed by two different methodologies: a coupled simulation of the flow and body motions (free motions) and a flow simulation with given forced motion. Two degrees of freedom – heave and pitch – in incident regular head waves were considered. For both cases the ”worst-case wave” for this vessel was computed beforehand with a linear panel method. This worst-case wave – wave length and height – was the only input for the coupled simulation of motions. The input for the forced-motion simulation was the wave plus the motion amplitudes and phases.

The numerical method is based on an extention of a Navier-Stokes code with a ”body motions module” to couple the fluid flow with the body motions induced by the flow and/or by external forces.

This allows to simulate unsteady ship motions in the 6 DOF. The methodology has been applied to several dynamic cases showing that large amplitude motions including capsizing, slamming, water entry, wave-piercing and water on deck can be simulated. The robustness of this methodology is mainly due to the simplicity of tracking the vessel's motions without deforming the numerical mesh or using complicated multi-mesh strategies. The VOF method in conjunction with a moving, rigid mesh attached to the vessel and suitable boundary conditions are shown to be very robust and efficient.

2. NUMERICAL METHOD

To couple the fluid flow and body motions I extended the Navier-Stokes solver COMET with a *body-motion module*. COMET is a commercial code developed in Germany by ICCM GmbH, now a member of the CD Adapco Group, the developers of the well-known multi-purpose STAR-CD code.

The general idea for coupling the fluid flow with the body motions is as follows: the Navier-Stokes flow solver computes the flow around the body in the usual way, taking into account the fluid viscosity, flow turbulence and deformation of the free surface. The forces and moments acting on the body are then calculated by integrating the normal (pressure) and tangential (friction) stresses over the body surface. Following this, the body-motion module solves the equations of motion of the rigid body in the 6 DOF using the forces and moments calculated by the flow solver as input data. The motion accelerations, velocities and displacements (translations and rotations) are obtained by integrating in time. The position of the body is updated and the fluid flow is computed again for the new position. By iterating this procedure over the time, the body trajectory is obtained.

2.1 BODY-MOTION MODULE

Two orthogonal Cartesian reference systems (RS) are used: A non-rotating, non-accelerating Newtonian RS (O, X, Y, Z) which moves forward with the mean ship speed, and a body-fixed RS (G, x, y, z) with origin at G, the centre of mass of the body. The undisturbed free-surface plane always remains parallel to the XY plane of the Newtonian RS. The Z-axis points upwards. The x-axis of the body-fixed RS is directed in the main flow direction, i.e. from bow to stern, the y-axis is taken positive to starboard and the z-axis is positive upwards. The body motions are executed using a *single-grid strategy*, where a rigid, body-fixed grid moves relative to the Newtonian RS, and the ficticious flow forces due to the grid movement are automatically taken into account in the flow equations. The body-motion module is linked and run simultaneously with the flow solver and can operate and update all flow variables, boundary conditions and parameters of the numerical method.

The motion of the rigid body in the 6 DOF are determined by integrating the equations of variation of linear and angular momentum written in the form referred to G (all vector components expressed in the Newtonian RS):

$$m\ddot{\vec{X}}_G = \vec{F} \qquad , \qquad \overline{\overline{T}}\,\overline{\overline{I}}_G\overline{\overline{T}}^{-1}\dot{\vec{\Omega}} + \vec{\Omega} \times \overline{\overline{T}}\,\overline{\overline{I}}_G\overline{\overline{T}}^{-1}\vec{\Omega} = \vec{M}_G \tag{1}$$

where m is the body mass, $\ddot{\vec{X}}_G$ the absolute linear acceleration of G, $\vec{F}$ is the total force acting on the body, $\dot{\vec{\Omega}}$ and $\vec{\Omega}$ are the absolute angular acceleration and angular velocity, respectively, and $\vec{M}_G$ is the total moment with respect to G, $\overline{\overline{I}}_G$ is the tensor of inertia of the body about the axes of the body-fixed RS, $\overline{\overline{T}}$ is the transformation matrix from the body-fixed into the Newtonian RS.

The contributions to the total force and to the total moment acting on G are:

$$\vec{F} = \vec{F}_{flow} + \vec{W} + \vec{F}_{ext} \qquad , \qquad \vec{M}_G = \vec{M}_{G_{flow}} + (\vec{X}_{ext} - \vec{X}_G) \times \vec{F}_{ext} \tag{2}$$

where $\vec{F}_{flow}$ and $\vec{M}_{G_{flow}}$ are the total fluid flow force and moment determined by integrating the normal (pressure) and tangential (friction) stresses, obtained from the Navier-Stokes solver. They include the static and the dynamic components of the water and of the air flow. $\vec{W}$ is the body weight force. $\vec{F}_{ext}$ can be any external force acting on the body which one wants to introduce to simulate for instance the towing forces and moments.

The vessel motions are described in each time instant by the position of its centre of gravity $\vec{X}_G$ and the body orientation given by $\overline{\overline{T}}$. Surge, sway and heave are defined in this work as the translations of G in the directions of the Newtonian RS. The angles of rotation are defined in the following order: First the rotation around the vertical axis in the Newtonian RS (yaw or leeway angle), second the rotation around the new transverse axis (pitch or trim angle), and last the rotation around the new longitudinal axis (roll or heel angle). To integrate in time the equations of motion a first-order explicit discretisation method has shown to work well and is used preferably. Instead of integrating the angular velocity $\vec{\Omega}$ to obtain the rotation angles, the new orientation of the body is found by integrating the unit vectors of the body-fixed RS, which are the columns of $\overline{\overline{T}}$. For details on the body-motion module see [1].

2.2 FLOW SOLVER

The solution method in COMET is of finite-volume-type and uses control volumes (CVs) with an arbitrary number of faces (unstructured meshes). It allows cell-wise local mesh refinement, non-matching grid blocks, and moving grids with sliding interfaces. The integration in space is of second order, based on midpoint rule integration and linear interpolation. The method is fully implicit and uses quadratic interpolation in time through three time levels.

The deformation of the free surface is computed with an *interface-capturing scheme* of VOF type (Volume Of Fluid), which has proven to be well suited for flows involving breaking waves, sprays, hull shapes with flat stern overhangs and section flare, etc. In this method, the solution domain covers both the water and air region around the hull and both fluids are considered as one effective fluid with variable properties. An additional transport equation for a void fraction of liquid is solved to determine the interface between the two fluids. The *High-Resolution-Interface-Capturing* (HRIC) discretisation scheme for convective fluxes in the void fraction equation is used to ensure the sharpness of the interface.

The solution method is of pressure-correction type and solves sequentially the linearised momentum equations, the continuity equation, the conservation equation of the void fraction, and the equations for the turbulence quantities. The linear equation systems are solved by conjugate gradient type solvers and the non-linearity of equations is accounted for by Picard iterations. The method is parallelised by domain decomposition in both space and time and is thus well suited for 3-D flow computation with free surfaces – especially when they are unsteady, as in the case of freely-floating bodies – since they require a lot of memory and computing time. For details on the flow solver see [3].

2.3 PREVIOUS APPLICATIONS AND VALIDATION

Resistance prediction with this method including the dynamic sinkage and trim (steady-state case) were validated for the Series 60 hull and for the model of a very fat ship with a blunt bow similar to a tanker (breaking-wave computations). These two examples showed that the method works well for very tiny changes in sinkage, trim (and also heel for the drift sailing condition) as well as for very large ones. The inclusion of the dynamic sinkage and trim in the calculations improved the agreement with experiments, and thus performance prediction.

Simulations of unsteady body motions were validated for 2-D drop tests with a wedge (used for slamming investigations). Comparisons with experiments proved very good agreement for both magnitude and timing of the accelerations, velocities and motions [1]. A validation for a 3-D case was also carried out for the model of a naval combatant in head waves and 2 DOF (heave and pitch) and showed good agreement with experiments. Slamming and green water on deck were simulated as well. In all these simulations the body trajectory, velocity and accelerations are obtained from the flow forces and/or external forces acting on the body without the need for prescribing the body trajectory.

The method has also been extensively applied to the steady flow around sailing yachts and for the simulation of the yachts responses to incident waves coming from any direction [2]. Furthermore, to planing crafts were investigated with this methodology [5], with the additional difficulty of the extremely high Froude numbers up to $F_n = 4$.

2.4 NUMERICAL MESH AND SIMULATION SET-UP

The shape of the vessel was delivered in an iges-file. This was modelled further (decks) together with the boundaries of the computational domain with the program Pro/Engineer and in the ICEM-CFD mesh generator. A numerical grid consisting of approximately 230 000 control volumes was generated using the HEXA module of ICEM-CFD. Only one side of the vessel was modelled and a symmetry plane was set at the centre-line plane. The computational domain extends for about $1.0\ D$ above deck and $1.0\ L_{oa}$ in front of the bow, behind the transom, below the keel and to the side. The mesh has such a large domain, especially above the deck, to allow large pitch motions in head waves. As turned out later, a still larger domain above the deck and a finer resolution below the keel would have been desirable.

The main dimensions of the vessel are shown in Table I and the environmental conditions – vessel speed and characteristics of the regular waves – are given in Table II.

Table I. Model data

lenght over all L_{oa}	71.00 m
water line lenght L_{wl}	62.50 m
breath B	13.50 m
draft d	3.70 m
depth D (bow)	11.00 m
mass m	1545.4 t
LCG (KG)	5.987 m
LCG-transom	30.037 m
pitch moment of inertia	486897 t m^2

Table II. Wave data and vessel speed

wave lenght λ_w	112.8 m
wave height H_w	7.0 m
wave direction μ	180° m (head waves)
vessel speed V_{see}	6.2 m/s, 12.0 kn
frequency of wave encounter ω_e	1.0845 s^{-1}
period of wave encounter T_e	5.7933 s
wave number k	0.0557 m^{-1}
wave steepness H_W/λ_W	$=0.062$

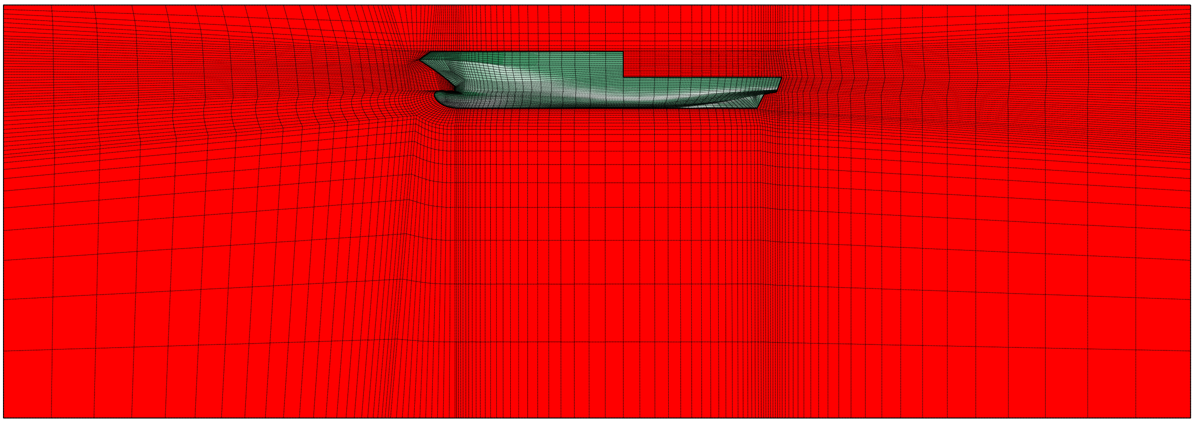

Figure 1. Numerical mesh around hull viewed from the side

Figure 1 shows the whole mesh viewed from the side and Figure 2 shows a close-up view of the bow region. The front, side, bottom and top flow-boundaries were specified as an inlet of constant known velocity (vessel speed in opposite direction plus orbital velocity of the incoming waves) and known void fraction distribution defining the water and air regions (wave elevation). The wake flow-boundary was specified as a zero-gradient boundary of known pressure distribution (hydrostatic pressure). All calculations were performed using the standard k-ϵ turbulence model with wall functions ($R_n : 3.46 \cdot 10^8$).

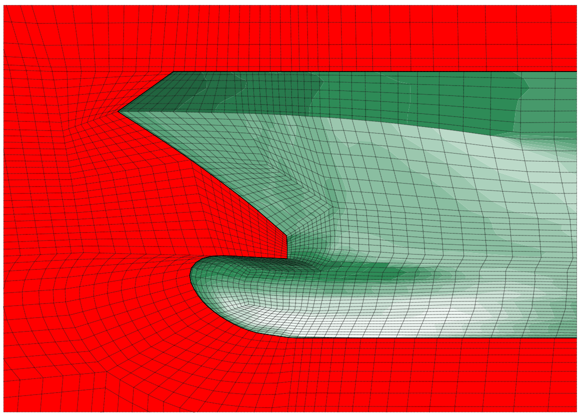

Figure 2. Numerical mesh around hull viewed from the front

3. COUPLED SIMULATION OF FREE MOTIONS IN INCIDENT HEAD WAVES

This work is based on prior simulations of ship responses to incident waves coming from different directions at moderate forward speed as well as at extremely high speeds up to $F_n = 4$. The results obtained were quite encouraging; some results could be successfully validated with model tests and others, for which no model tests were available, showed plausible qualitative results. However, the challenge the present simulations constituted were due to the very large pitch amplitude and the occurrence of slamming and large amounts of water on deck due to the very steep waves.

The incident waves are generated at the inlet flow-boundary by imposing the instantaneous wave elevation and orbital velocities according to the (linear) Airy-theory. The orbital velocities of the waves are superimposed on the mean flow velocity. Three wave parameters are set at the beginning of a simulation: The wave amplitude ζ_w, the wave length λ_w and the wave direction μ relative to the vessel course ($\mu = 0°$ means from astern and $\mu = 90°$ from port). Due to numerical diffusion the wave amplitude hitting the vessel is reduced to some extent, although the used VOF-method produces surprisingly good results on relatively coarse meshes.

The wave steepness in this case ($H_W/\lambda_W = 0.062$) is beyond the scope of validity of the Airy-theory (up to $H_W/\lambda_W = 0.010$). This means that due to numerical and natural diffusion the wave shape in the simulations substantially varies from the sinus wave and tends to adopt the shape of a natural wave.

Figure 3 shows two snap-shots during a simulation as the vessel slams into a head wave. The figures also show the edges of the computational domain and the cut of the computational domain with the undisturbed waterplane. In the single-grid strategy used in these simulations, the computational domain moves as a whole relative to this plane. The boundary conditions – the mean flow velocity, the orbital velocity, the void fraction distribution defining the wave elevations, the turbulence parameters and so on – have to be very carefully imposed at each time instant relative to the undisturbed waterplane. The VOF method and the implemented boundary conditions have proven to be very robust, since the free surface can leave the computational domain in any place, i.e. through the top flow-boundary as shown in the figure to the right as is the case when the vessel pitches with a large angle. Even the simulation of capsizing upside down is possible.

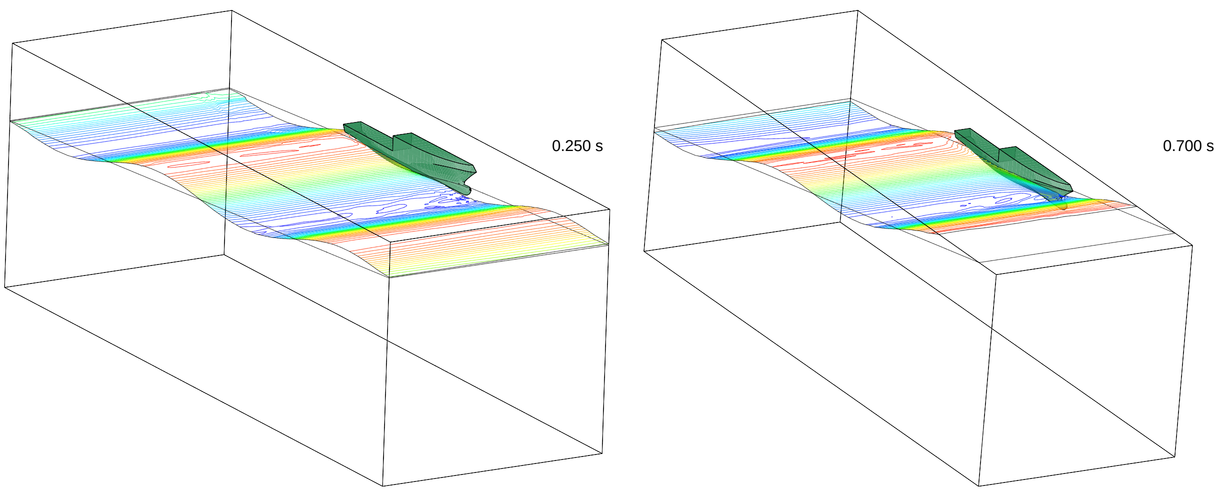

Figure 3. Two time instants in the simulation. Edges of the computational domain and undisturbed waterplane

3.1. CALM WATER AS INITIAL CONDITION

Figures 4, 5 and 6 show the time history of motions (heave, pitch), motion velocities (heave velocity and pitch angular velocity) and forces (resistance, heave force and pitch moment) for the case of the simulation initialised at $t=0$ with full forward speed in calm water. At $t=0$ the waves start to generate at the inlet boundary of the computational domain. After 4 to 5 wave encounter periods the waves hitting the vessel have developed their full size and the motions, velocities and forces are periodical and in this case slightly non-sinusoidal. The pitch motion is strongly damped, as was expected, due to the slamming forces when the bow penetrates the wave. A minimum of 9.2° is reached, whereas when the vessel's bow rises out of the water the motion is less damped and a maximum of 11.1° is reached. The heave motion is more symmetrical.

Unfortunately, the simulated wave elevation could not be monitored, since no wave gauge has been implemented so far. But for the sake of comparison a theoretical sinus wave (wave elevation at the location of G) with the same frequency and phase as in the simulation is depicted in Figure 4. Taking the zero-crossing of the pitch motion as a reference, the simulation yield that the wave is 0.53 rad and the heave motion 0.82 rad out of phase (delayed).

The motion amplitudes were made non-dimensional by dividing the maximum minus the minimum heave amplitude by the wave height and by dividing the maximum minus the minimum pitch angle by the (linear) wave slope double amplitude. The following values were obtained. They are in the usual range found for similar types of vessels and speeds:

$(\zeta_{max}-\zeta_{min})/H_w=0.88$

$(\theta_{max}-\theta_{min})/kH_w=0.91$

3.2. SINUS WAVE AS INITIAL CONDITION

Since the simulated wave shape departs from the theoretical sinus wave shape and is to some extent reduced in amplitude (negative more than positive) due to a rather coarse grid below the keel, a simulation initialised with a sinus wave extending over the whole computational domain was performed. Figures 7, 8 and 9 are the counterparts of 4, 5 and 6, but for the simulation with the sinus wave as initial condition. To avoid problems starting the simulation, the initial condition was chosen at the instant when the vessel is on an even keel, coming down from the positive heave and pitching down by the bow into the next wave. The initial conditions – heave $\zeta=+3.653$ m, heave velocity $w=-3.9$ m/s, pitch angular velocity $r=-0.23$ rad/s, and wave phase $\alpha_{wave}=0.59$ rad – were taken as given by the motion prediction with the panel code GL-PANEL. They were then the same as used for the forced-motion simulation which will be presented below. The motions, velocities and forces are then slightly larger for the first wave period but after 3 to 4 periods they are basically the same as those from the simulation started in calm water.

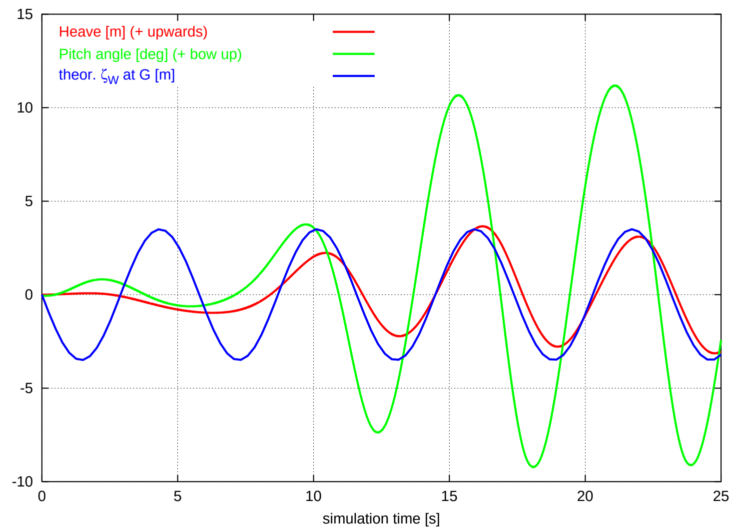

Figure 4. Motions: free-motion simulation, calm water as initial condition

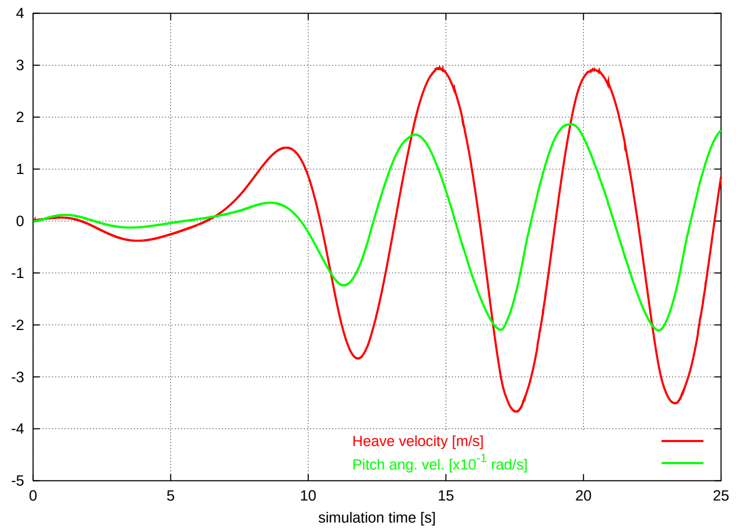

Figure 5. Motion velocities: free-motion simulation, calm water as initial condition

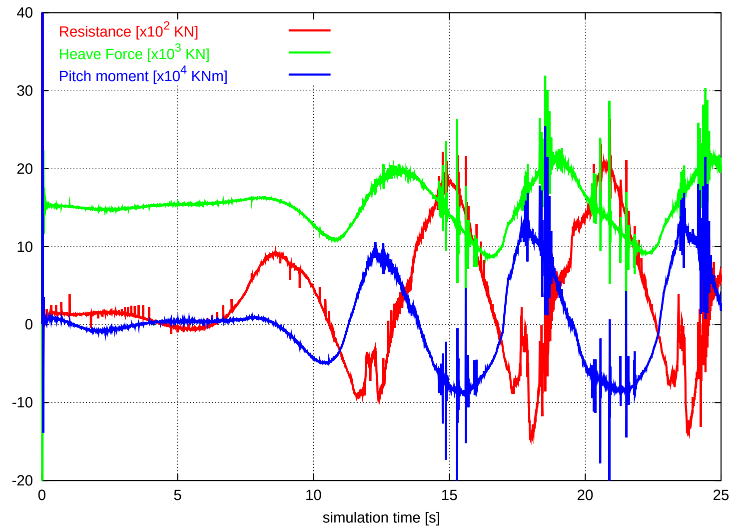

Figure 6. Forces and moments: free-motion simulation, calm water as initial condition

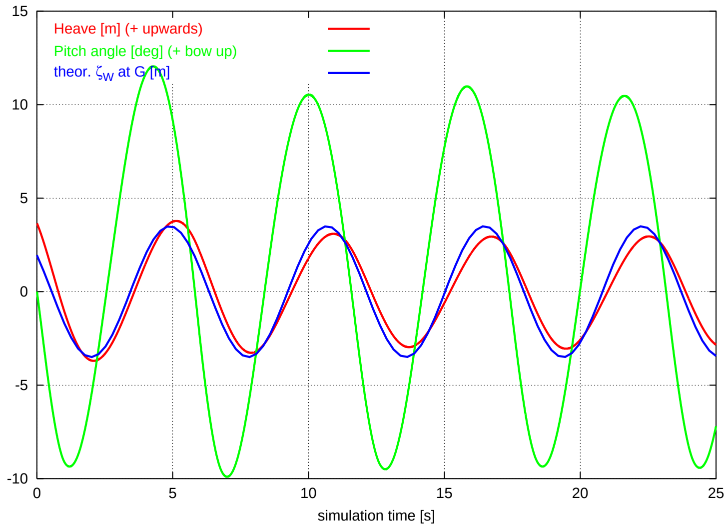

Figure 7. Motions: free-motion simulation, sinus wave as initial condition

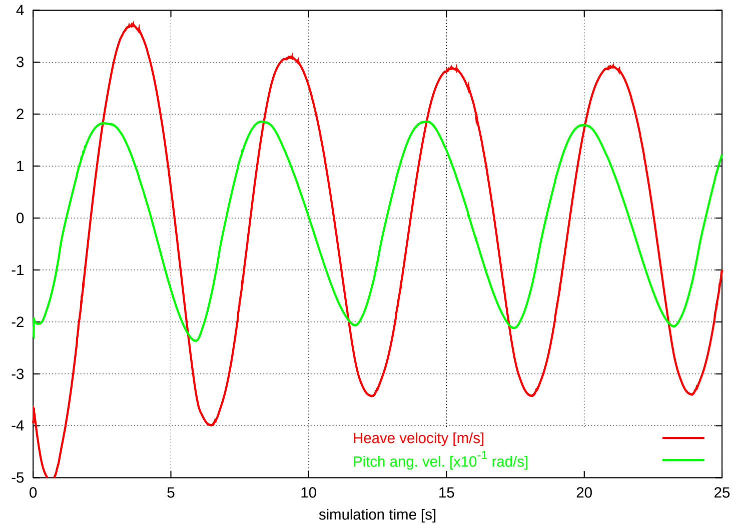

Figure 8. Motion velocities: free-motion simulation, sinus wave as initial condition

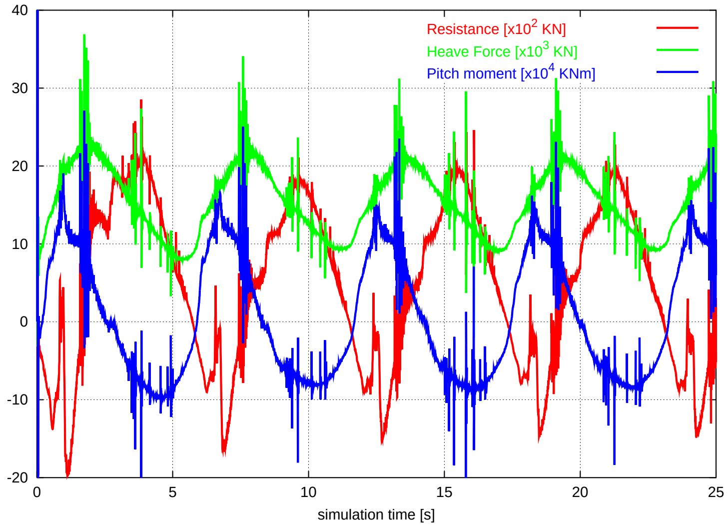

Figure 9. Forces and moments: free-motion simulation, sinus wave as initial condition

4. SIMULATION OF FORCED MOTIONS IN INCIDENT HEAD WAVES

Prior to running these RANSE simulations, a study of the vessel's motions with a panel method (program GL-PANEL) was performed at Germanischer Lloyd in order to find the 'worst-case wave' which would yield the largest slamming pressures to be expected. Then, a RANSE simulation with forced motions in that wave was also performed with the aim of comparing the predicted slamming forces with the free-motion simulations presented above. The forced motions were given by GL-PANEL as harmonic functions and were shifted to avoid problems starting the simulation to zero pitch angle for $t=0$:

Heave [m]	$\zeta = 5.17\, sin(-\omega_e t + 0.79)$
Pitch [deg]	$\theta = 12.6\, sin(-\omega_e t + 0.0)$
Wave elevation [m]	$\zeta_w = 3.5\, sin(-\omega_e t + 0.59)$

Figure 10 compares the motions for the forced-motion case (thin lines) with the free motions (thick lines) of the simulation started in calm water for the last wave period and shifted so that they coincide in pitch phase. From this figure is obvious that the amplitudes in the free motion simulation are much more damped than those predicted by GL-PANEL. Moreover, the pitch motion in the free-motion simulation strongly depart from the sinusoidal shape. The phases of the heave motion relative to the pitch motion are almost the same for the RANSE and GL-PANEL simulations. Figure 11 compares the GL-PANEL motions with those of the simulation initialised with a sinus wave and the same motion position and velocities.

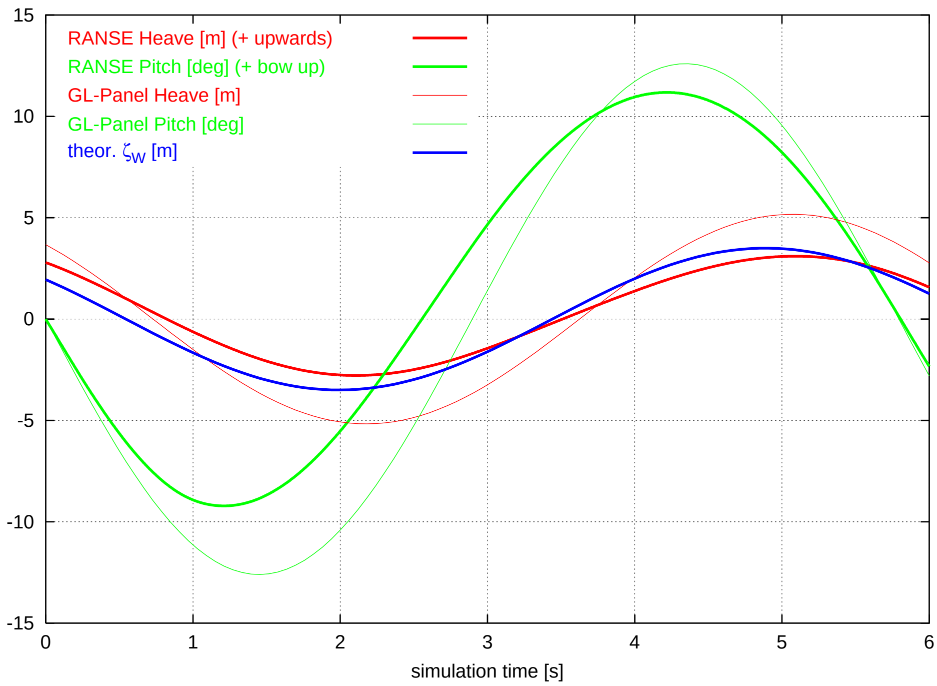

Figure 10. Comparison of motions from GL-PANEL and RANSE simulation initialised in calm water

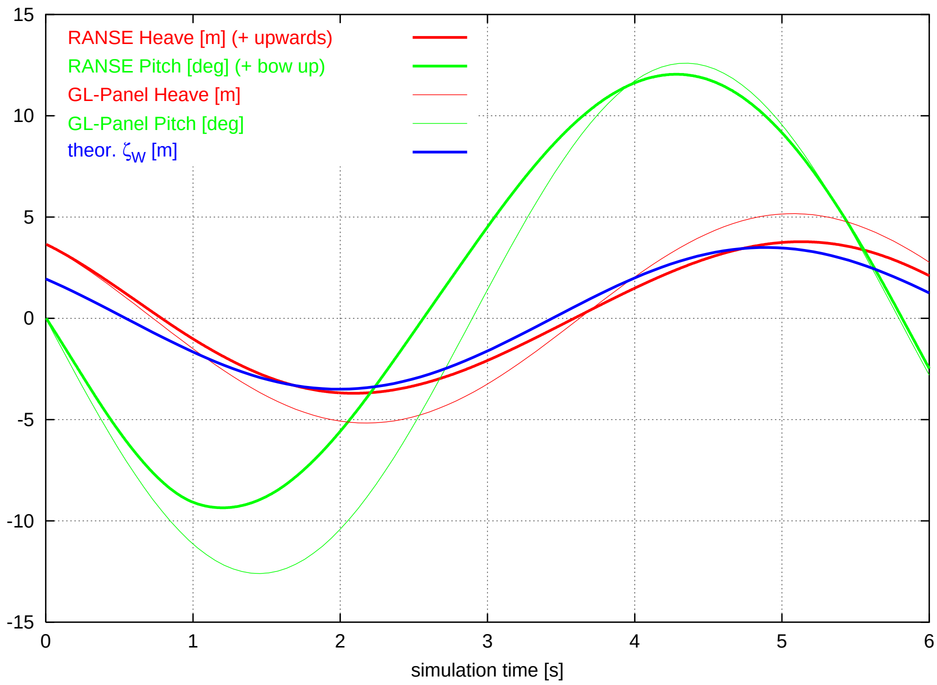

Figure 11. Comparison of motions from GL-PANEL and RANSE simulation initialised with sinus wave

5. SLAMMING PRESSURES

For calculating the slamming pressures at the required zones of the flared bow, a user-programmed routine was used which runs at the beginning of the simulation and finds the region elements of the numerical mesh which fall inside the given zones or panels and saves them to a file. This file is then read when restarting the simulation and the region numbers are kept in a common block between iterations. In each iteration an average of the pressure in each panel is calculated by taking into account the contributions of all regions belonging to that panel The averaged pressures are then written to a file for monitoring purposes.

Table III gives the coordinates of the given zones in the coordinate system of the iges-file containing the hull shape. Panel 5 was not required but added for comparison. Figure 12 shows the region elements found for each panel, together with lines indicating the coordinates of the panels.

Figures 13 and 14 show the averaged pressures on the five panels for the first and the third half periods (bow below the water) respectively, as predicted by the free-motions simulation initialised with the sinus wave. After 3 periods the maximum or peak of the averaged pressures basically do not change anymore. The same pressures are also predicted by the free-motion simulation initialised with calm water after the motions are periodic (4 to 5 wave periods).

Figures 15 and 16 show the averaged pressures also for the first and the third half periods respectively, but this time as predicted by the forced-motion simulation initialised with the sinus wave.

Table III. Definition of pressure monitoring panels

Panel #	X-transom [m]	Z-keel [m]	Area [m^2]
Panel 1	61.75 – 62.40	5.0 – 5.3	0.193
Panel 2	61.10 – stem	4.4 – 5.8	4.529
Panel 3	59.15 – 61.10	3.6 – 5.8	5.017
Panel 4	57.20 – 59.15	4.4 – 5.8	4.496
Panel 5	64.40 – 62.00	keel – 0.5	1.671

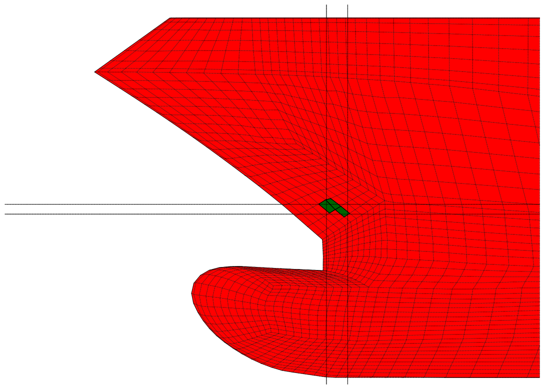

Panel 1

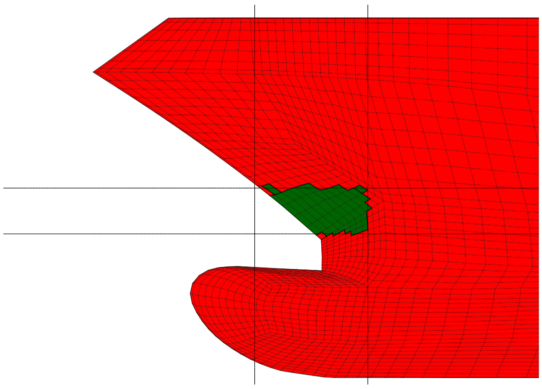

Panel 2

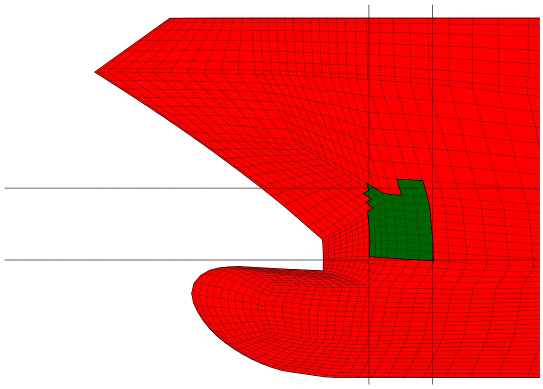

Panel 3

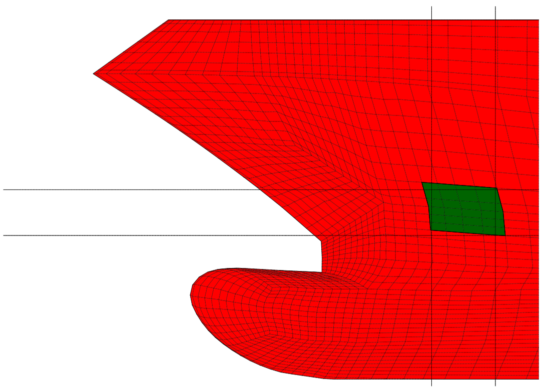

Panel 4

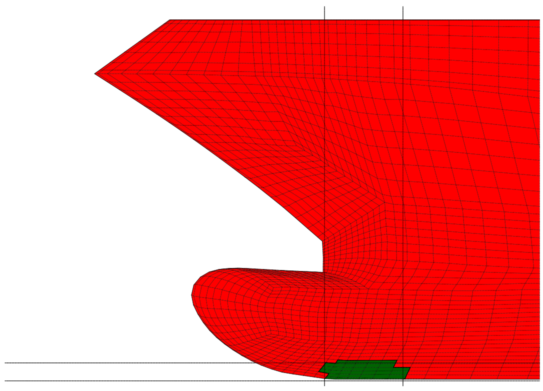

Panel 5

Figure 12. Region elements (in green) defining the panels for slamming pressure monitoring. Lines indicate the required zones

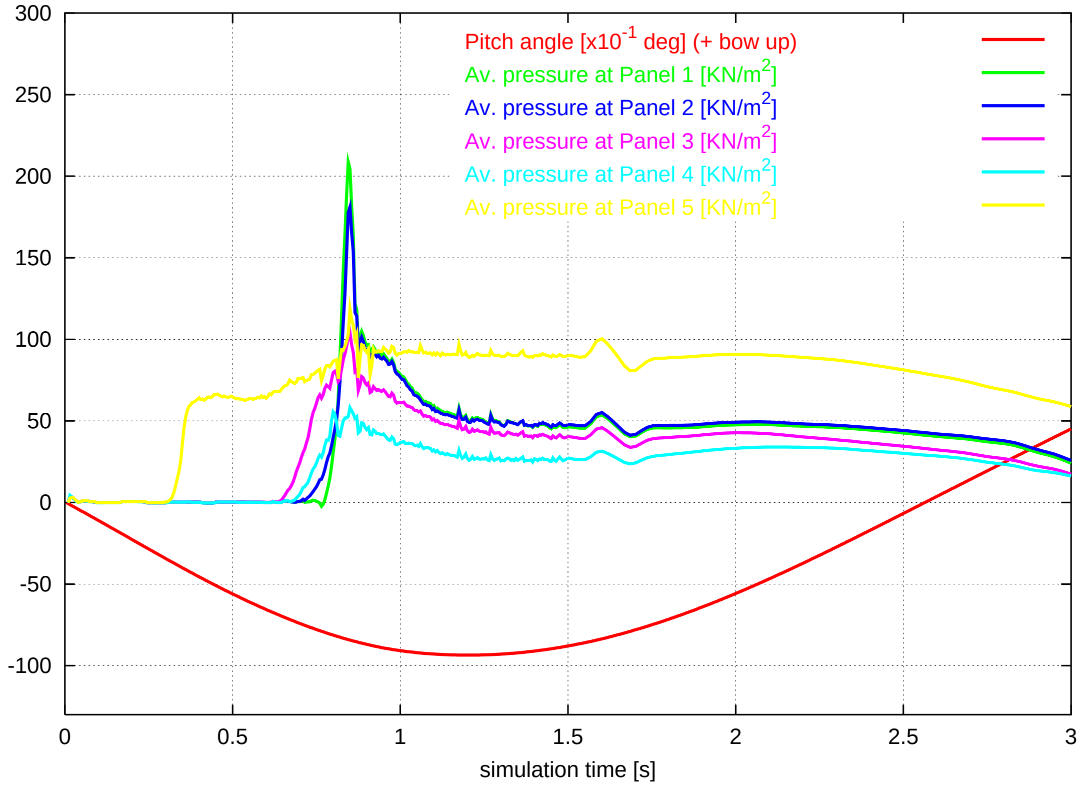

Figure 13. Averaged slamming pressures: free-motion simulation in first half period after initialisation

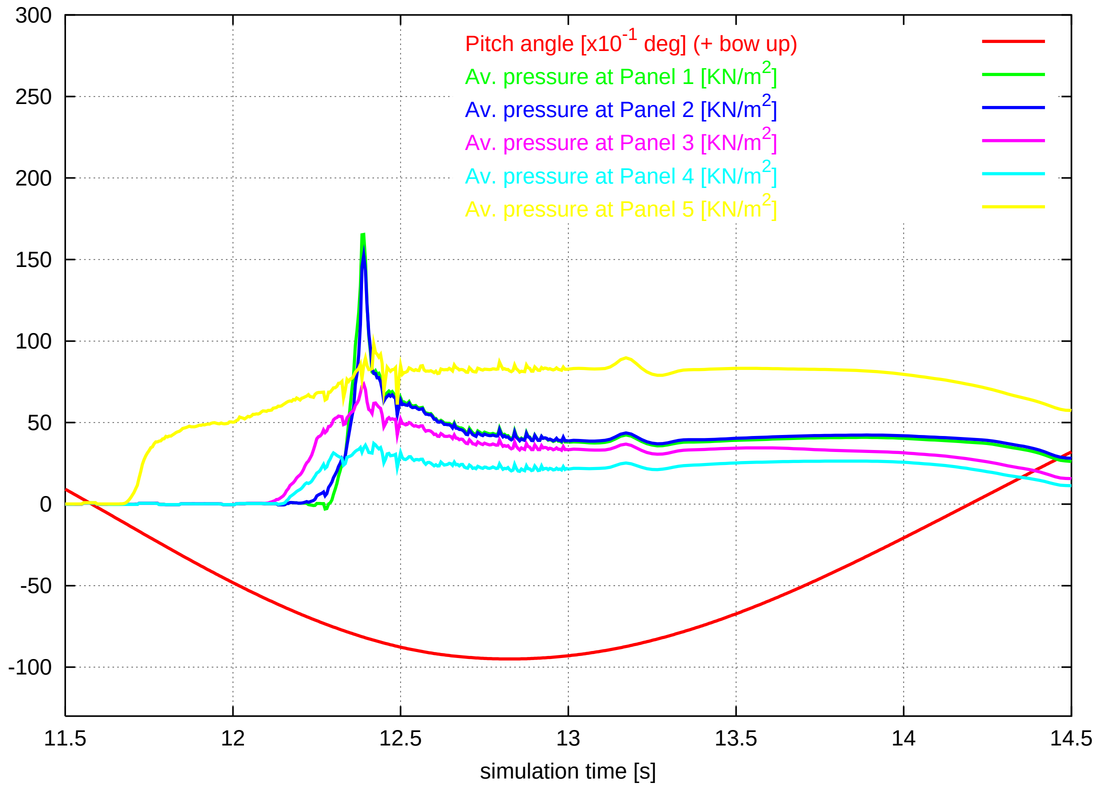

Figure 14. Averaged slamming pressures: free-motion simulation in third half period

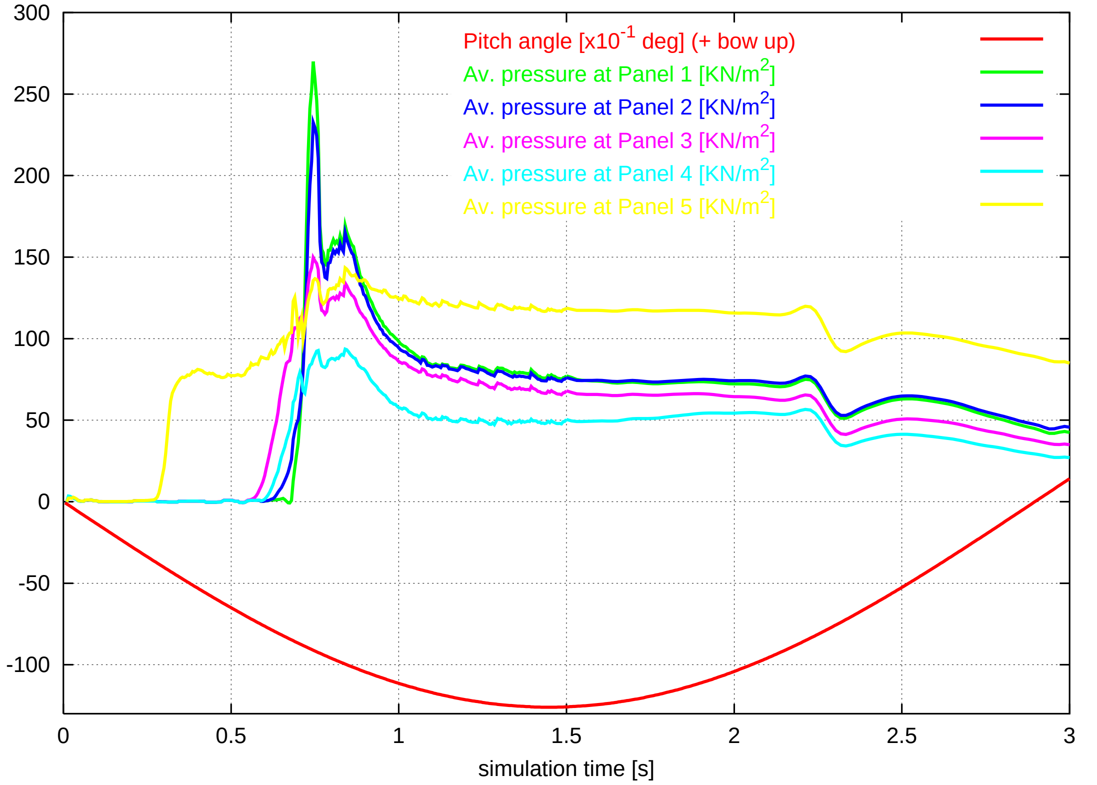

Figure 15. Averaged slamming pressures: forced-motion simulation in first half period after initialisation

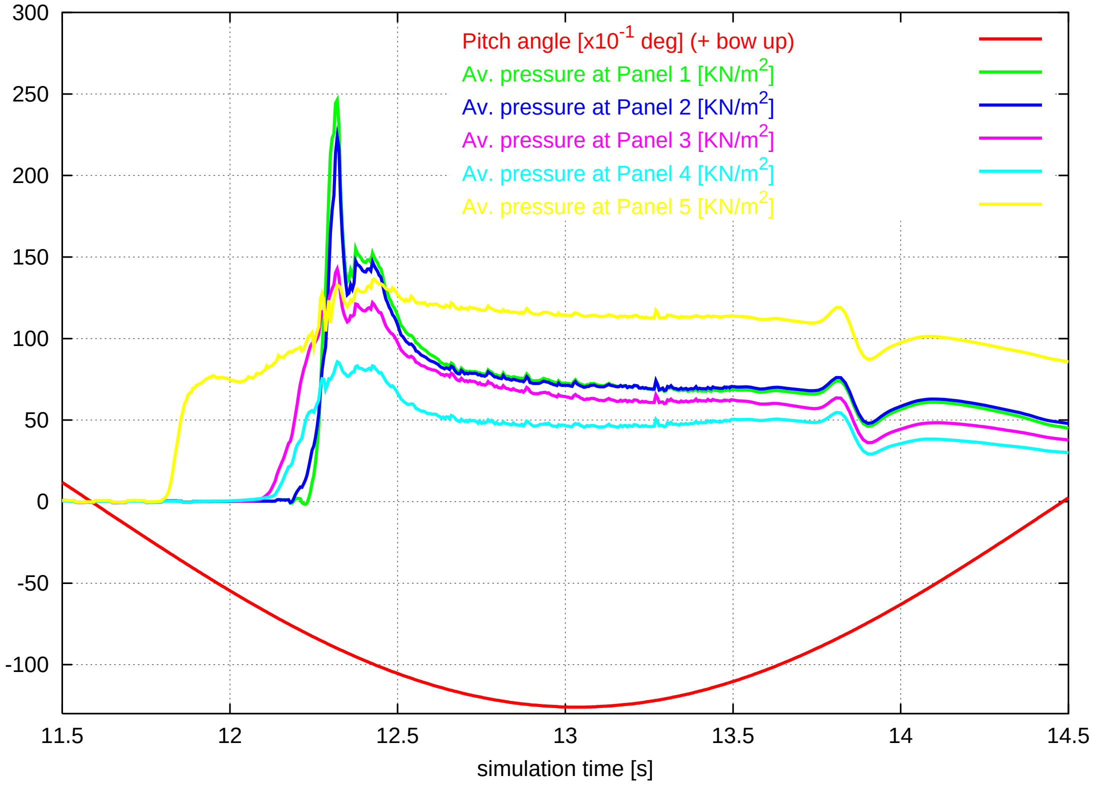

Figure 16. Averaged slamming pressures: forced-motion simulation in third half period

6. CONCLUSIONS

References

[1] Azcueta, R., *”Computation of Turbulent Free-Surface Flows Around Ships and Floating Bodies”*, PhD. thesis, Technical University Hamburg-Harburg, 2001.

[2] Azcueta, R., *”RANSE simulations for sailing yachts including dynamic sinkage & trim and unsteady motions in waves”*, High Performance Yacht Design Conference Auckland, 2002.

[3] Ferziger, J. H. & Perić, M., *Computational Methods for Fluid Dynamics*, Springer, Berlin, 1996.

[4] Katayama, T., Hinami, T. & Ikeda, Y., ”Longitudinal motion of a super high-speed planing craft in regular head waves”, *4th Osaka Colloquium on Seakeeping Performance of Ships*, 2000.

[5] Caponnetto, M., Söding, H. & Azcueta, R., ”Motion Simulations for Planing Boats in Waves”, *Ship Technology Research*, to be published 2003.